Stability of mixed convection flow

K. Muralidhar*† and F. A. Kulacki*‡

Hydrodynamic and thermal stability of a confined stratified flow is analyzed by means of linearized perturbation theory. A numerical procedure, which has generality with respect to boundary conditions, Reynolds number, Prandtl number, mean velocity, and temperature profiles, is described to solve the Orr-Sommerfeld problem altered by buoyancy. Two test cases—the study of transition of plane Poisseulle flow affected by stable and unstable stratification and the stability of flow generated by a wall heater with and without superimposed flow—have been solved, demonstrating the power and generality of the technique. A wide range of mixed convection problems has also been covered in this paper, and interesting Prandtl number effects have been observed. In the case of stratified Poisseulle flow, increasing Prandtl number significantly reduces the influence of buoyancy. Moreover, for stability of flow over a wall heater, higher values of Prandtl number strongly amplify the effect of prescribed flow.

Keywords: *linear stability; mixed convection; modified Orr-Sommerfeld equations; orthonormalization; Eigen values; critical Reynolds number; critical Rayleigh number*

Introduction

The hydrodynamic and thermal stability of stratified, confined laminar flows has been considered in this study. These include the case of nonisothermal plane Poisseulle flow weakly affected by buoyancy and the other extreme case of buoyant flow from a horizontal wall heater, modified by a superimposed stream. Stability analysis has been carried out within the framework of linear perturbation theory. A numerical method is used to determine the most destabilizing eigenvalue whose imaginary part represents the disturbance amplification and that does not have computational difficulty when the Reynolds and Rayleigh numbers are large. Moreover, the method is a general one with respect to Prandtl number, mean velocity, temperature profiles, and boundary conditions. The scope of the physical problems dealt with is intended to demonstrate the usefulness of this technique for a wide range of mixed convection problems.

Stability of stratified channel flows has been considered earlier by Gage and Reid.[1] Their work involves a complete analytical solution under restrictive conditions such as unity Prandtl number. Platten and Legros[2] have considered stability under a variety of circumstances, including channel flow and free and mixed convection problems. They further described experiments performed to demonstrate and locate the point of transition. Hwang and Cheng[3] have studied the problem of onset of longitudinal vortices in fully developed channel flow heated from below. Kamotani, Ostrach, and Miao[4] have performed experiments to measure augmentation in heat transfer in the poststability regime for flow in a horizontal channel whose lower wall is heated. Gebhart[5] has provided a comprehensive review of stability of free convective, external flows.

The objective of this work is twofold. First, a versatile numerical technique with a wide range of applicability has been used. Second, attention has been focused on certain interesting and yet unsolved problems in the area of stratified flows; two broad cases have been considered:

1. Stable and unstable stratified plane Poisseulle flow
2. Onset of convection and stability of free and mixed convective flow over a wall heater

In both cases, Prandtl number effects have also been studied.

* Department of Mechanical and Aerospace Engineering, University of Delaware, Newark, DE 19716, USA
† Presently at Lawrence Berkeley Laboratory, California, USA
‡ Presently at Colorado State University, Colorado, USA
Received 2 October 1986 and accepted for publication 23 April 1987

0142-727X/87/030228-07$3.00

Formulation

The equations governing the growth of disturbances small enough to justify linearization can be obtained by perturbing the momentum and energy equations of the instantaneous flow field. The onset of instability studied here is marked by the appearance of transverse rolls. The specific form of the fluctuations is taken as periodic, as required by normal mode analysis. The stability of plane Poisseulle flow is investigated using two-dimensional perturbations, whereas for the wall heater problem, both two- and three-dimensional perturbations lead to the same form of governing equations. For the hydrodynamic stability problem, Squire's theorem guarantees that two-dimensional disturbances would be more destabilizing than three-dimensional ones. Its extension to buoyancy-affected problems is assumed here. For a horizontal configuration of the channel, this leads to the following system of equations (Platten and Legros[2]). Two different Reynolds numbers (Re_1 and Re_2) have been defined for cases 1 and 2 to conform to existing practice in literature.

Case 1: plane Poisseulle flow

$$L_4\phi = \mathrm{Ri}_b\theta \tag{1}$$

$$L_2\theta = \bar{\theta}'\phi \tag{2}$$

where

$$L_4 \equiv (i\alpha\,\mathrm{Re}_1)^{-1}(D^2-\alpha^2)^2-(U-c)(D^2-\alpha^2)-\bar{\xi}_y$$

and

$$L_2 \equiv (i\alpha\,\mathrm{Re}_1\,\mathrm{Pr})^{-1}(D^2-\alpha^2)-(U-c)$$

In Equation 1, Ri_b is the bulk Richardson number of mean flow (independent of Re_1) and is a prescribed quantity. The complex wave speed, c, is given as

$$c = c_r + ic_i \tag{3}$$

Written in this form, the smallest of Re_1 that makes $c_i > 0$ is the critical value for the problem and a criterion for instability.

Case 2: flow over a horizontal wall heater

$$L_4\phi = \mathrm{Ra}\,\alpha^2\theta \tag{4}$$

$$L_2\theta = \bar{\theta}'\phi \tag{5}$$

where

$$L_4 \equiv D^4 - [i\alpha(\mathrm{Re}_2\, U - c) + 2\alpha^2]D^2 - [i\alpha^3(\mathrm{Re}_2\, U - c) + \alpha^4 - i\alpha\, \mathrm{Re}_2\, \bar{\xi}_y]$$

and

$$L_2 \equiv D^2 - (\alpha^2 - i\alpha c\, \mathrm{Pr} + i\alpha\, \mathrm{Pr}\, \mathrm{Re}_2\, U)$$

In Equations 4 and 5, U is prescribed, and the smallest Ra that makes $c_i > 0$ is the critical value of transition.

In deriving Equations 1–5, x derivatives of the base flow velocity fields are assumed small in comparison to the y derivatives only to the extent that they isolate the stability equations in x and y directions. Further, stability of a given y-dependent mean flow is considered, assuming the flow system would break down first because of severe gradients in this direction. This can be expected to be valid for the case of a horizontal infinite channel.

For both of these cases, the following homogeneous boundary conditions are assumed to hold on the solid boundaries. These correspond to zero velocities and fixed mean temperatures on the walls of the channel.

$$\phi = D\phi = 0 \qquad \theta = 0 \tag{6}$$

Specification of base flow and temperature

The mean flow that undergoes transition has been taken as two-dimensional, steady, and incompressible, except for the density dependence on temperature in the body force terms.

Case 1: plane Poisseulle flow (Figure 1a)

Fully developed laminar flow (plane Poisseulle flow) in a horizontal channel is considered here. Superimposed on the velocity field is a thermal field, as obtained from the mixing of two parts of equal velocity streams at initially different temperatures. This leads to a thermal mixing layer at their interface, along the center of the channel, whose thickness grows with the location along the channel length. Typical profiles of mean velocity and temperature are shown in Figure 1(a). The following corresponding formulas have been used:

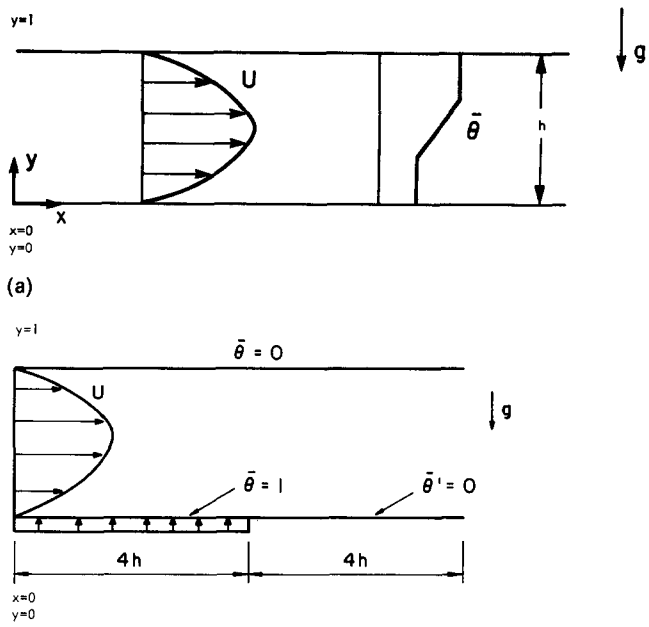

Figure 1 (a) Configuration of stratified plane Poisseulle flow; (b) fully developed flow over a wall heater of finite length

$$U = 1 - (2y-1)^2 \tag{7}$$

$$\begin{aligned} \bar{\theta}' &= 0 && 0 < y\,0.4 \\ &= \pm 5.0 && 0.4 < y\,0.6 \\ &= 0 && 0.6 < y\,1.0 \end{aligned} \tag{8}$$

Notation

a_i, b_i	Complex column vectors
$\bar{b}_i$	Complex conjugate of b_i
B	Transfer matrix
c	Eigenvalues, s^{-1}
c_r, c_i	Real and imaginary parts of c
$\bar{D}$	Complex determinant
F_1, F_2	Real and imaginary parts of $\bar{D}$
g	Gravitational acceleration, m/s^2
h	Channel height, m (also characteristic length)
i	Imaginary unit, $\sqrt{-1}$
L_2, L_4	Differential operators
Pr	Prandtl number, ν/α_f
p	Number of orthonormalizations
Ra	Rayleigh number of base flow, $g\beta\Delta T h^3/\nu\alpha_f$
Re_1	Reynolds number, $U_{max}h/2\nu$
Re_2	Reynolds number, $U_m h/\nu$
Ri_b	Bulk Richardson number, $g\beta\Delta T h/2U_m^2$
t	Time, s
T	Disturbance temperature, °K
$\bar{T}$	Mean temperature, °K
ΔT	Bulk temperature difference, $\bar{T}_H - \bar{T}_C$
u, v	Disturbance speed in x and y directions
U, V	Velocity of base flow in x and y directions, m/s
x, y	Dimensionless physical coordinates
α	Wave number
α_f	Thermal diffusivity of the fluid, m^2/s
β	Volumetric expansion coefficient, °K^{-1}
ϕ	Amplitude function of ψ
$D\phi$	$d\phi/dy$
θ	Amplitude function of T
$\bar{\theta}$	Temperature field of base flow, $(\bar{T}-\bar{T}_C)/(\bar{T}_H-\bar{T}_C)$
$\bar{\theta}'$	$d\bar{\theta}/dy$
ν	Kinematic viscosity, m^2/s
ψ	Disturbance steam function
$\bar{\xi}$	Vorticity of mean flow field, $\partial V/\partial x - \partial U/\partial y$

Subscripts

c	Critical value
max	Maximum value
m	Mean value
H	Hot stream or boundary
C	Cold stream or boundary

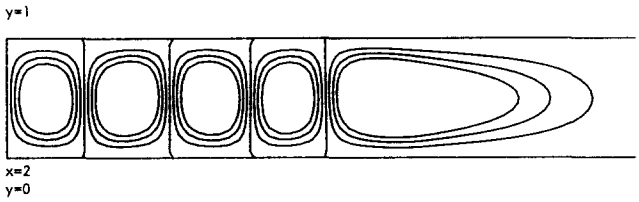

Figure 2 Streamlines in one half a horizontal channel with lower wall partially heated ($Re_2=0$, Pr=1, Ra=10,000)

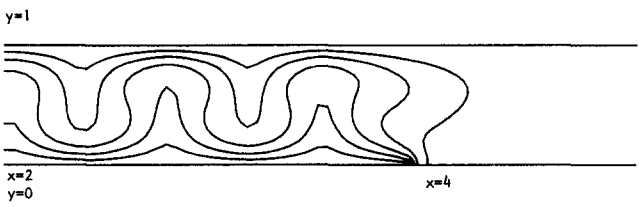

Figure 3 Isotherms in one half a horizontal channel with lower wall partially heated ($Re_2=0$, Pr=1, Ra=10,000)

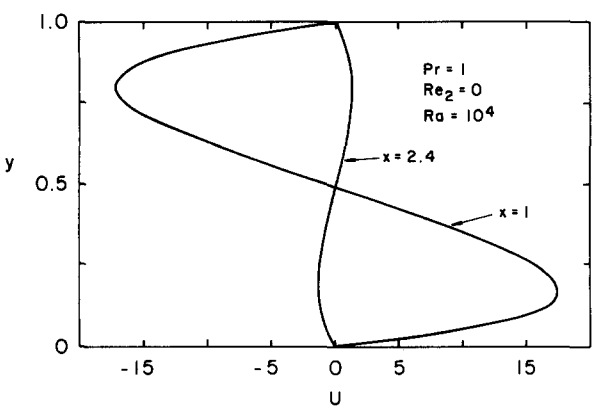

Figure 4 Base velocity profile in laminar buoyant convection in a horizontal channel arising from a partially heated lower wall

Flow fields like these are encountered in air-conditioning applications, where fresh outside air is mixed with cooler recycled air. The positive sign refers to stable stratification of density, and the negative sign, to the unstable case. Buoyancy is included to the extent that fluctuations introduced in the channel are promoted in an unstable density configuration, or damped in other cases. This, in effect, is the case of weak mixed convection, where the mean flow field is affected by gravitational effects only to a minor extent.

Case 2: flow over a wall heater (Figure 1b)

Flow due to a heater located on the lower wall of a horizontal channel and flow over it are studied here. Flow systems like these are encountered in cooling of electronic equipment and are characterized by a strong interaction between the velocity and temperature distribution. This, forced flow distorting a buoyancy-driven flow field, is the other extreme and is classified as the case of strong mixed convection.

The velocity and thermal fields generated by a wall heater located in an infinite, horizontal channel have been obtained by solving the unsteady Navier-Stokes and energy equations by finite differences (Roache[6] and Nguyen *et al.*[7]). The numerical scheme uses the second upwind procedure, and steady state is obtained by marching in time. Figures 2 and 3 show the roll pattern and isotherms when $Ra=10^4$ and the lower wall of the channel is partially heated. The heater length is four times the channel height. For the free convection problem, it is sufficient to consider only half the heater length by virtue of the available symmetry. For the mixed convection problem, with prescribed fully developed flow, the full heater length has been included. Figures 4 and 5 show base velocity and temperature profiles when $Pr=1$, $Re_2=0$, and $Ra=10^4$, and Figures 6 and 7 show the same when $Re_2=20$. Similar results have been obtained for $Pr=10$.

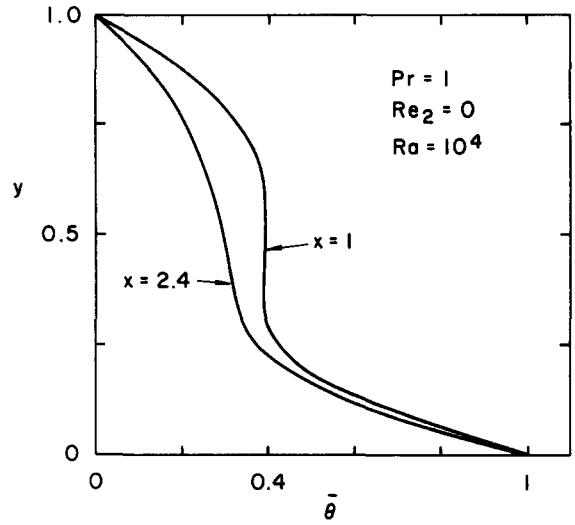

Figure 5 Base temperature profile in laminar buoyant convection in a horizontal channel arising from a partially heated lower wall

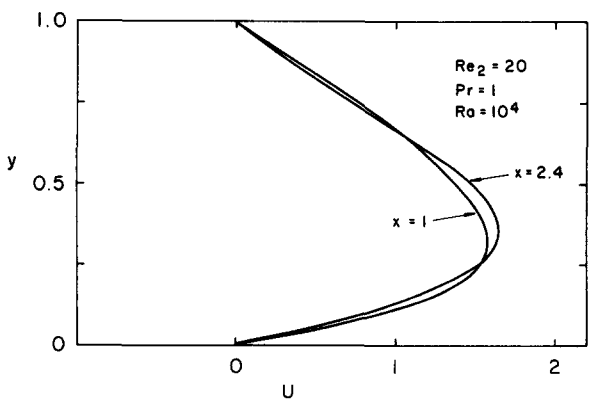

Figure 6 Base velocity profile in mixed convection in a horizontal channel with a partially heated lower wall

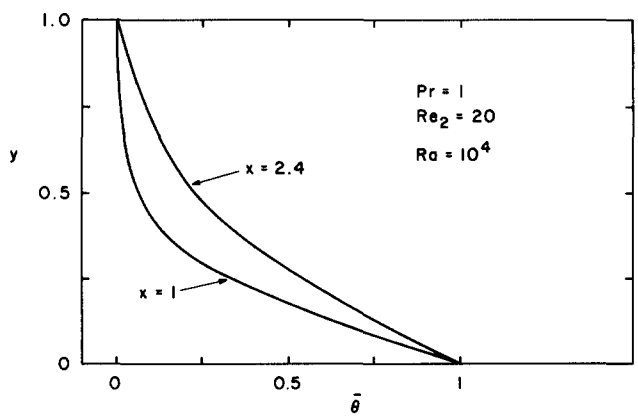

Figure 7 Base temperature profile in mixed convection in a horizontal channel with a partially heated lower wall

Solution procedure

Equations 1, 2, 4, 5, and 6 constitute an eigenvalue problem, with α, Re, Ra, and Ri_b as parameters and c as the eigenvalues that provide nontrivial solutions to the stability problem. The solution scheme adapted to the present problem is called the direct integration method (Davey[8]). The robust nature of this class of techniques has been demonstrated rigorously by Meyer.[9] By straightforward Runge-Kutta integration, one can establish the following matrix relation:

$$\begin{bmatrix} \phi \\ D\phi \\ D^2\phi \\ D^3\phi \\ \theta \\ D\theta \end{bmatrix} = \begin{bmatrix} \cdot & X & X & \cdot & X \\ \cdot & X & X & \cdot & X \\ \cdot & \cdot & \cdot & \cdot & \cdot \\ \cdot & \cdot & \cdot & \cdot & \cdot \\ \cdot & X & X & \cdot & X \\ \cdot & \cdot & \cdot & \cdot & \cdot \end{bmatrix} \begin{bmatrix} \phi \\ D\phi \\ D^2\phi \\ D^3\phi \\ \theta \\ D\theta \end{bmatrix} \qquad (9)$$

$y=2 \qquad y=0$

The complex 6×6 transfer matrix can be obtained columnwise by solving six initial value problems with the vector $(\phi, D\phi, \ldots, D\theta)^T_{y=0}$ assuming values $(1, 0, \ldots, 0)$ and so on to $(0, 0, \ldots, 1)$. The boundary conditions are then imposed on this matrix equation. For a nontrivial solution, the determinant $\bar{D}$ formed by the X's must vanish. For a given α and Re (or Ra), the quantity c is adjusted so that this determinant is close to zero, that is, c is the root of the determinant. Root finding can then be done by a variety of schemes (for example, Muller's method). Alternatively, one can prescribe α and $c_i = 0$ and solve for two roots, Re (or Ra) and c_r. This can be carried out by a Newton-Raphson scheme. This approach was found to be quite efficient and will be described later.

Orr-Sommerfeld problems exhibit matrix ill conditioning when cast in the form of Equation 9. This is due to widely varying growth rates of the independent solutions, which leads to inaccurate evaluation of the ill-formed determinant through round-off errors. The numerical scheme used here eliminates this problem by an orthonormalization technique. Instead of integrating all the way to the next wall, a series of subtransfer matrices is formed by integration from $y=0$ to $y=y_1$, y_1 to y_2, and so on. If these transfer matrices are denoted at $B_1, B_2, \ldots, B_p$, the overall transfer matrix is

$$B = B_p B_{p-1} \ldots B_1 \qquad (10)$$

To avoid ill conditioning, the matrix obtained after every multiplication has columns 3, 4, and 6 orthogonalized with respect to one another and all columns normalized after that. The definition of orthogonal columns used here is as follows. If $\sum_{i=1}^{6} a_i b_i = 0$, then a and b are orthogonal normal. This follows from the unusual inner product $(a, b) = \sum_{i=1}^{6} a_i b_i$ rather than $\sum_{i=1}^{6} a_i \bar{b}_i$ which makes c, the wave speed, an analytic function of $\bar{D}$ from standard root finding techniques to apply.

To determine the roots of the matrix in Equation 9, c_i is set to zero, and α is specified as a parameter. Then, c_r and Re (at the critical value) are the unknown roots to be obtained from the simultaneous equations,

$$F_1 \equiv \text{real}(\bar{D}) = 0 \qquad (11a)$$

$$F_2 \equiv \text{imaginary}(\bar{D}) = 0 \qquad (11b)$$

where F_1 and F_2 are implicity functions of c_r and Re. Corrections required over the initially assumed values of c_r and Re are given by

$$\Delta \text{Re} = \left(F_2 \frac{\partial F_1}{\partial c_r} - F_1 \frac{\partial F_2}{\partial c_r} \right) F^{-1}$$

$$\Delta c_r = \left(F_1 \frac{\partial F_2}{\partial \text{Re}} - F_2 \frac{\partial F_1}{\partial \text{Re}} \right) F^{-1} \qquad (12)$$

and

$$F = \frac{\partial F_1}{\partial \text{Re}} \frac{\partial F_2}{\partial c_r} - \frac{\partial F_1}{\partial c_r} \frac{\partial F_2}{\partial \text{Re}}$$

The derivatives in Equation 12 are easily computed by finite differences.

Results and discussion

A step size of 0.001 has been used for the fourth-order Runge-Kutta integration, and p has been taken as 8. Size convergency for smaller step sizes and larger p has been observed in all calculations. Prandtl numbers ranging from 0.1 to 10 have been used in this study, but the method of obtaining eigenvalues is general enough for any finite Prandtl number, as well as a variety of temperature profiles. Values of critical Reynolds number and Rayleigh number represent convergence to the second decimal place, whereas those of c_r are correct to the fourth decimal place. The critical Reynolds of unstratified plane Poisseulle flow calculated in this work ($Re_{1c} = 5762.7$) agrees well with the value obtained by Thomas[10] ($Re_{1c} = 5780$). Further validation of the numerical scheme is described later in the context of thermal stability.

Case 1

Stability results for stratified Poisseulle flow are given in Figures 8–11. For stable stratification, the critical Reynolds number increases as Ri_b increases. This is particularly so when $Pr \leq 1$, whereas for $Pr = 10$, the critical Reynolds number is virtually unchanged for $0 < Ri_b < 0.1$. The flow thus becomes increasingly stable because of the increased resistance of a high Prandtl number fluid to sustain fluctuations in the presence of a buoyancy field. As viscous effects start to predominate over diffusive ones ($Pr > 1$), these increasingly govern the growth of fluctuations, and the stability characteristics tend to the case of zero buoyancy. The temperature profile considered here cannot lead to complete laminarization (as observed in the work of Gage and Reid[1]) because Ri is locally zero outside the thermal mixing layer. The stable region of the flow field lies outside the stability envelope and can be seen in the familiar plot or Re versus the wave number α (Figure 9). As Ri_b is increased to 0.1,

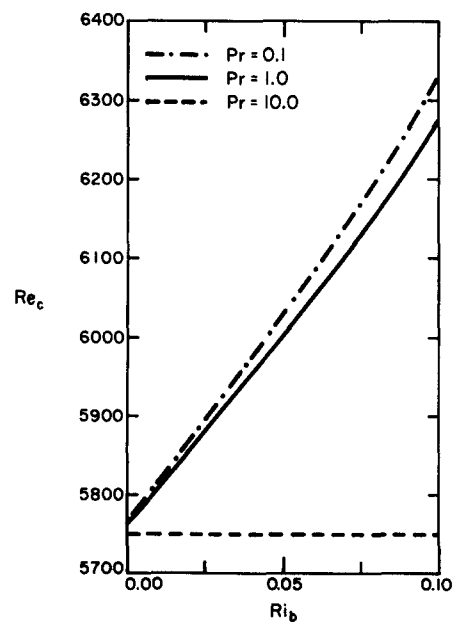

Figure 8 Effect of bulk Richardson number on critical Reynolds number—stable stratification

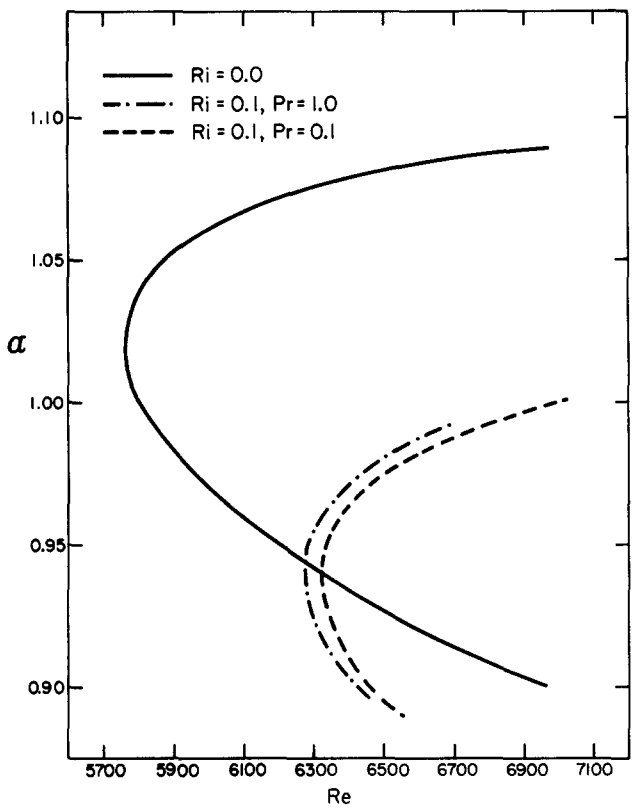

Figure 9 Stability envelopes in stably stratified flow

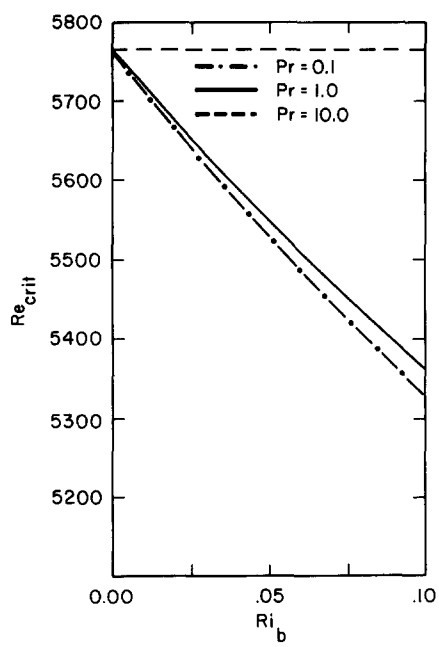

Figure 10 Effect of bulk Richardson number on critical Reynolds number—unstable stratification

the two branches of the envelope collapse, and this can be interpreted as increased stability of flow.

When the flow is unstably stratified in density, it is possible to lower the critical Reynolds number in weak mixed convection problems if it is assumed vortex rolls due to thermal instability do not appear first. This can certainly be anticipated for the values of Reynolds number used in this work. Figure 10 shows the drop in the values of Re_{1c} as a function of bulk Richardson number for various values of Pr. This result corresponds to an imposed temperature profile, as in Figure 1(a), but in an unstable configuration (Equation 8). As seen earlier, lower values of Pr experience a stronger influence of buoyancy. For values of Pr greater than 10, this influence is insignificant. Figure 11 shows the stability envelopes of buoyancy-affected flow, where the reduced stability of flow for higher values of Ri_b is evident from its expanding interior region.

Case 2

Figure 12 shows the results for onset of convection for flow over a horizontal wall heater. The velocity field is chosen as fully developed, and the temperature gradient is unity across the channel height. This can be physically realized in a wind tunnel with a linearly heated grid. The critical Rayleigh number marks the point of thermal instability for both flow and no-flow conditions. Table 1 shows detailed results for this case, and the

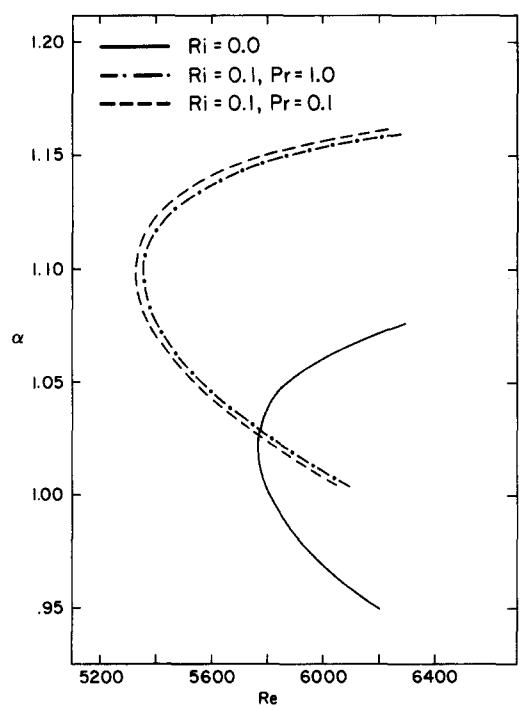

Figure 11 Stability envelopes in unstably stratified flow

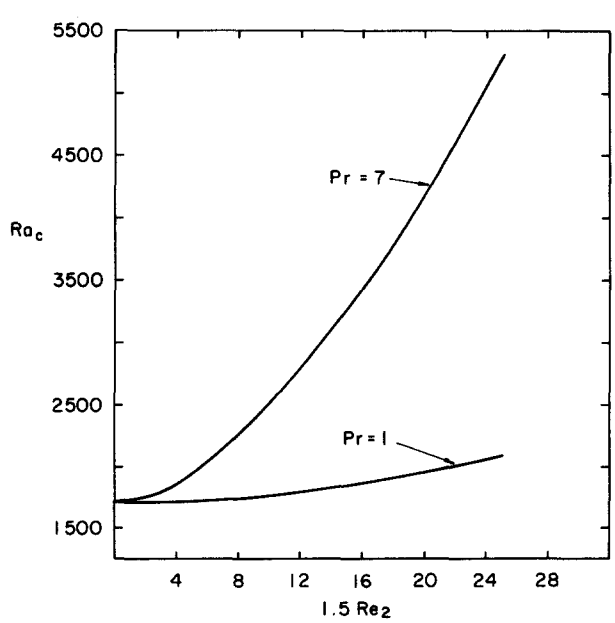

Figure 12 Critical Rayleigh number at onset of convection

Table 1 Effect of Re_2 on Ra_c at onset of convection

Pr	Re_2	Ra_c	α_c	c_r
1	0	1707.8	3.12	0
1	6.67	1766.8	3.12	7.799
1	16.67	2082.8	3.16	19.46
7	0	1707.8	3.12	0
7	2	1793.6	3.08	2.59
7	4	2030.5	3.01	5.1738
7	8.33	2871.1	2.95	10.8715
7	13.33	4178.1	2.99	17.525
7	16.67	5276.0	3.0	21.93

Table 2 Stability results for free and mixed convection flow over a wall heater

Re_2	Pr	x	Ra_c	α_c	c_r
0	1	1	3.386 E+05	8.5	−9.6862
0	1	2.4	3.325 E+05	9.72	+0.05346
20	1	1	5.59 E+05	8.75	19.893
20	1	2.4	2.646 E+05	10.175	19.394
0	10	1	4.248 E+05	10.0	−1.588
0	10	2.4	3.37 E+05	9.74	−0.03629
20	10	1	∞		
20	10	2.4	∞		

values for Pr = 7 agree closely with those given by Platten and Legros.[2] For $Re_2 = 0$, c_r is calculated as zero, which is the "exchange of stabilities" principle. It can also be seen that the numerical scheme correctly brings out the absence of a dependence of Ra_c on Pr when $Re_2 = 0$. However, for $Re_2 > 0$, higher values of Pr strongly amplify the effects of prescribed flow by delaying the point of transition.

When the Rayleigh number associated with the heated surface is greater than the critical value, a base flow field is established that could undergo a series of discrete transitions toward turbulence. Figures 4–7 show the base flow velocity and temperature profiles obtained by a finite difference scheme for $Ra = 10^4$ and Pr = 1. Table 2 gives the critical Rayleigh numbers at which these profiles would allow the growth of small periodic fluctuations. It can be seen that, for $Re_2 = 0$ and Pr = 1, the disturbance wave velocity could be either in the positive or negative direction, depending on the location along the heater length. However, when $Re_2 = 20$, the waves are convected along the mean flow. For $Re_2 = 0$, the critical Rayleigh number is relatively unaltered from $x = 1$ to $x = 2.4$ and is about 3.3×10^5. For $Re_2 = 20$, there is continuous decrease in Ra_c as x increases, since in this case, the thickness of the thermal boundary layer increases in the same direction. For the Reynolds number used here, this reduction occurs even beyond the value obtained for purely free convective flow. This result needs further validation from experiments. Figure 13 shows the stability envelopes for free convective flow over the wall heater at two x locations, when Pr = 1 and $Re_2 = 0$.

When Pr = 10, free convective phenomena exhibit instability in much the same way as for Pr = 1. However, for $Re_2 = 20$, the critical Rayleigh number becomes far too high to be realized in practice. This, marked ∞ in Table 2, means the flow cannot be destabilized by means of heating alone. The only instability that can occur in a case like this is the viscous shear type, as discussed in case 1.

The problem of onset of instability considered in this work has implications in engineering practice. These points of transition indicate an increase in complexity of the flow pattern, resulting in both an increase in pressure drop and heat transfer rates. Study of stratified flow (Figure 1a) shows that a stable temperature gradient increases the critical Reynolds number, thus delaying the point at which the hot and cold streams start to mix vigorously by means of turbulent motion. In an air-conditioning system, this could mean mechanical failure arising from severe thermal stresses related to the difference in temperatures. On the other hand, when the stratification improves mixing, it simultaneously increases pressure drop or reduces flow rates for a given rating of the pumping unit.

The second flow configuration considered here (Figure 1b) has applications in cooling of electronic equipment. As the surface temperature of a panel is allowed to increase, the performance of the electronic system is adversely affected, though at certain critical points ($Ra_c \approx 3 \times 10^5$), the complex flow pattern results in elevated heat transfer rates. By a proper choice of fluid properties, this surface temperature can be made small enough not to deteriorate system behavior. If this cannot be realized, the alternative is to use superimposed flow over the heated surfaces. Results obtained in this paper show that enhancement due to gravity effects are possible for air ($Pr \approx 1$), whereas they are negligible for fluids like water ($Pr \approx 10$).

The use of linear stability theory restricts this study to the region very close to transition of a flow state. As the flow pattern departs from this point, the approximation of small perturbation is no longer valid. Hence for any practical application, stability results also have to be supplemented by solving full momentum and transport equations. When these equations are solved numerically, the stability analysis, which identifies the possibility of transition, can prove to be invaluable.

Conclusions

The hydrodynamic and thermal stability of a flow field have been studied at both limits of small buoyancy effect on forced flow and small superimposed flow on strong buoyant convection. The eigenvalue problem resulting from linear analysis has been solved by a numerical scheme general enough to handle a wide range of parameters, such as Re, Pr, and Ri, and also a variety of base flow profiles. Results show that in weak mixed convection problems, the ability of stratification to promote or suppress instability depends on the Prandtl number. At values of $Pr \geq 10$, this influence is seen as negligible,

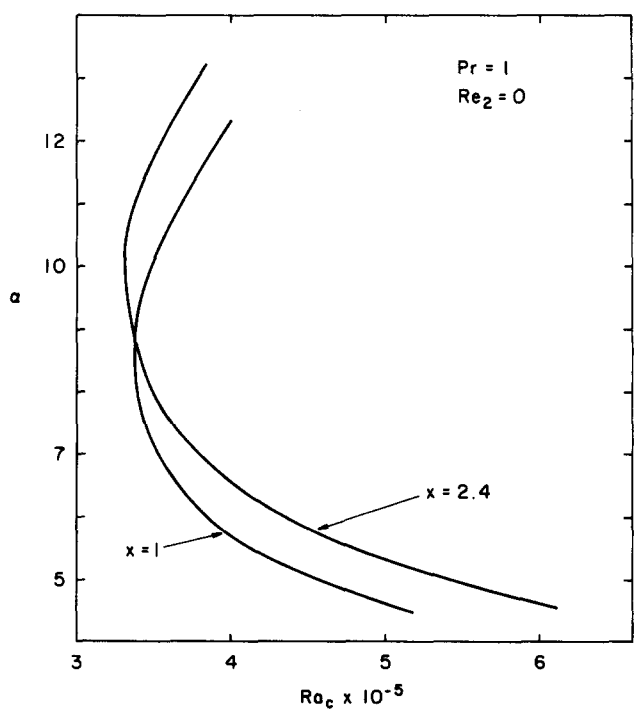

Figure 13 Stability envelope for free convection over a partially heated wall

increasing as Pr is reduced. This trend of thermal effects becoming secondary as Pr is raised is also observed at the other extreme of onset of convection in a bottom heated channel, in the presence of forced flow. However, flow generated by buoyancy shows only a small stability dependence on Pr (Ra_c being close to 3.5 E+05). The response of this flow system reverts rapidly to that of channel flow, even at low Reynolds numbers (≈ 20), and for Pr = 10, the possibility of thermal stability is eliminated ($Ra_c \rightarrow \infty$).

References

1 Gage, K. S., and Reid, W. H. The stability of thermally stratified plane Poisseulle flow. *J. Fluid Mech.*, 1968, **33**, 21–32.

2 Platten, J. K., and Legros, J. C. *Convection in Liquids*. Springer-Verlag, New York, 1984.

3 Hwang, G. J., and Cheng, K. C. Convective instability in the thermal entrance region of a horizontal parallel-late channel heated from below. *ASME J. Heat Trans.*, 1973, 72–77.

4 Kamotani, Y., Ostrach, S., and Miao, H. Convective heat transfer augmentation in thermal entrance regions by means of thermal instability. *ASME J. Heat Trans.*, 1979, **101**, 222–226.

5 Gebhart, B. Instability, transition and turbulence in buoyancy-induced flows. *Annual Review of Fluid Mech.*, 1973, 213–246.

6 Roache, P. J. *Computational Fluid Dynamics*. Hermosa Publishers, Albuquerque, 1976.

7 Nguyen, T. V., Maclaine-Cross, I. L., and de Vahl Davis, G. The effect of free convection on entry flow between horizontal parallel plates. Chapter 6 in *Numerical Methods in Heat Transfer*, ed., Lewis, R. W. John Wiley & Sons, New York, 1981.

8 Davey, A. A simple numerical method for solving Orr-Sommerfeld problems. *Quar. J. Mech. and Applied Math.*, 1973, **26**, 401–411.

9 Meyer, G. H. Continuous orthonormalization for boundary value problems. *J. Computation Phys.*, 1986, **62**, 248–262.

10 Thomas, L. H. A simple numerical method for solving Orr-Sommerfeld problems. *Quar. J. Mech. and Applied Math.*, 1973, **26**, 401–411.